NAIC-ID(RS)T-0382-94

NATIONAL AIR INTELLIGENCE CENTER

MODULATION EFFECT OF A BRAGG ACOUSTO-OPTIC BISTABLE SYSTEM

by

Zheng Zhiren, Gao Jinyue

HUMAN TRANSLATION

NAIC-ID(RS)T-0382-94 10 November 1994

MICROFICHE NR: 94C000470

MODULATION EFFECT OF A BRAGG ACOUSTO-OPTIC BISTABLE SYSTEM

By: Zheng Zhiren, Gao Jinyue

English pages: 11

Source: Guangxue Xuebao, Vol. 10, Nr. 1, January 1990; pp. 7-13

Country of origin: China
Translated by: Leo Kanner Associates
F33657-88-D-2188
Quality Control: Nancy L. Burns
Requester: NAIC/TATA/J.M. Finley

PREPARED BY:

TRANSLATION SERVICES
NATIONAL AIR INTELLIGENCE CENTER
WPAFB, OHIO

GRAPHICS DISCLAIMER

All figures, graphics, tables, equations, etc. merged into this translation were extracted from the best quality copy available.

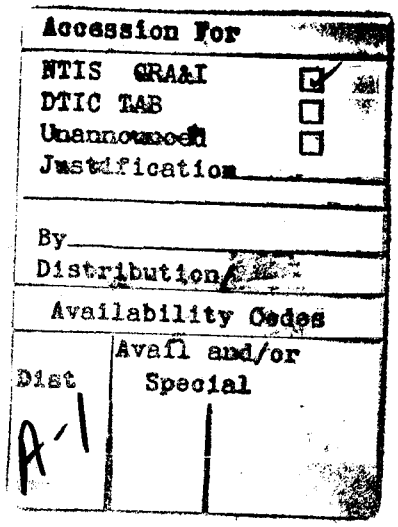

MODULATION EFFECT OF A BRAGG ACOUSTO-OPTIC BISTABLE SYSTEM

ZHENG ZHIREN and GAO JINYUE
Physics Department, Jilin University, Changchun
Submitted March 3, 1989. Edited draft received June 13, 1989

In this paper, the linear stability and the modulation effect of a Bragg acousto-optic bistable system are analyzed. According to the dynamic and stationary equations describing the system, the boundary for instability has been calculated. When the input intensity undergoes a sinusoidal modulation, we predict the resonance and shift of resonance peak of the output intensity in the stable region and the appearance of frequency looping phenomena in the unstable region.

I: INTRODUCTION

Acousto-optic bistable systems not only possess those qualities common to optical bistable system but also possess the characteristics of dual channel or multiple channel and ease of integration. In specific installations, its bistabilty and unstability are also different in a number of ways from electro-optic bistable systems. It is a system with widespread uses in optical communications and optical computers.

Chrostowski et al[1,2] have reported on experiments with Bragg acousto-optic bistable stationary equipment and Jerominek et al[3] and Dong Xiaoyi et al[4] have reported on dynamic characteristics of Roman-Nath acousto-optic bistable equipment. These articles emphasized reporting on the stable and non-stable characteristics of acousto-optic bistable systems. This article will discuss more systematically the time of linear stability of the Brag acousto-

optic bistable system, concentrating on a discussion of the modulation effect of that system.

II: DYNAMIC EQUATIONS

The Bragg acousto-optic bistable system depicted in Figure One can be described in the following equations[5]:

$$u_1(t) = \alpha' I K \sin^2[\pi/u_\pi(u_2(t)+u_0)], \quad (1)$$

$$\tau\, du_2(t)/dt + u_2(t) = \beta'[u_1(t-\tau_D)] \quad (2)$$

In these equations, $u_1(t)$、$u_2(t)$、u_0、u_π、I、α'、β'、K、τ、τ_D respectively indicate the light output electrical conversion voltage, the post amplification conversion voltage, the DC bias, the half-wave voltage, the input light intensity, the photo-electrical conversion coefficient, the voltage amplification multiple, the acousto-optic crystal diffraction efficiency, the reaction time of the feedback channel and the delay time. After appropriate substitution, the above formulas may be written in a non-dimensional form as:

$$I_2(t) = I_1 K \sin^2[V(t)+\theta], \quad (3)$$

$$dV(t)/dt + V(t) = I_2(t-T), \quad (4)$$

wherein $I_2(t) = \pi\beta' u_1(t)/u_\pi$, $I_1 = \pi\beta'\alpha' I/u_\pi$, $\theta = \pi u_0/u_\pi$,
$V(t) = \pi u_2(t)/u_\pi$, $T = \tau_D/\tau$, $t = t/\tau_0$

Substituting equation (3) into equation (4), we obtain]

$$dV(t)/dt + V(t) = I_1 K \sin^2[V(t-T)+\theta], \quad (5)$$

This is the dynamic equation of the Bragg acousto-optic bistable system.

Fig 1: Diagram of Bragg Acousto-optic Device.

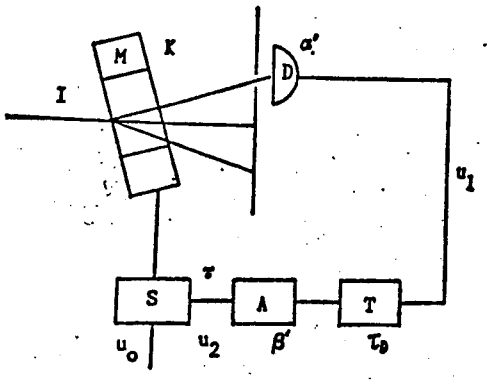

M is modulation device, D optic-electric detector, T delay sytem, A amplifier and B ultrasonic driving source.

Fig. 2. Curve of Stability State.

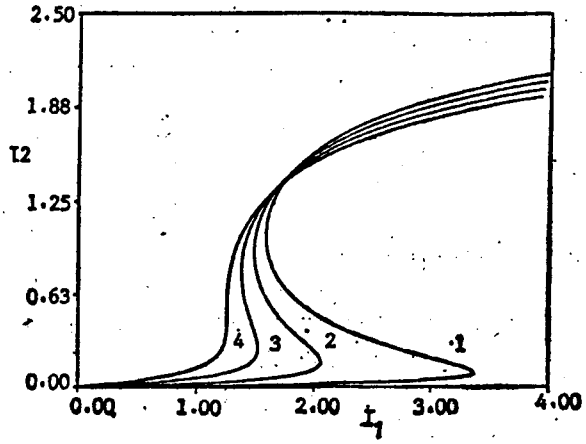

The parameters used here are K=0.8, Curves 1, 2, 3, and 4 correspond to θ=0.3, 0.5. 0.7 and 0.9 seconds respectively.

III: QUALITATIVE ANALYSIS OF BISTABILITY AND LINEAR STABILITY

In order to analyze the stability characteristics of this system, in equation (4) we set $dV(t)/dt=0$, obtaining $V(\infty)=I_2(\infty)$, changing equation (3) to

$$I_2=I_1K\sin^2(I_2+\theta). \qquad (6)$$

This is the dynamic equation of the Bragg Acousto-optic bistable system. Within an appropriate range of values for θ, there is bistability between the output I_1 and the input I_2. In equation

(6) if we set $dI_1/dI_2=0$, , we obtain

$$2I_2=\mathrm{tg}(I_2+\theta). \tag{7}$$

From equation (7) we obtain the range of values of θ for the bistability of the system as

$$n\pi<\theta<n\pi+\left(\frac{\pi}{4}-\frac{1}{2}\right)\approx n\pi+0.091\pi,\ (n=0,\ \pm1,\ \pm2,\ \cdots). \tag{8}$$

Figure Two represents a fur line bistability graph when the values of θ are $0.03\pi、0.05\pi、0.07\pi、0.09\pi$.

In order to analyze the dynamic stability, employing equation (5) near the point of stability, and solving for linear items, we obtain

$$\alpha+1=W\exp(-\alpha T)\cos\beta T, \tag{9}$$

$$\beta=-W\exp(-\alpha T)\sin\beta T, \tag{10}$$

$$W=2I_2/\mathrm{tg}(I_2+\theta), \tag{11}$$

Here, α and ß are the strong and weak portions of the linear eigenvalues, with α representing the amplitude gain and ß representing the oscillation frequency. W is the state parameter. By analyzing equations (9), (10) and (11), we can reach the following conclusions concerning linear stability:

(1). When W>1, and $dI_2/dI_1<0$ corresponds to the imaginary slope portions of the bistability graph. When W<1, dI_2/dI_1 corresponds to the real slope portions of the bistability graph.

(2). The points on the branches of the negative slope lines on the bistability graph are all unstable points ($\alpha>0$), and the points on the positive slope branches corresponding to W<1 are stable points ($\alpha<0$).

(3). The stability of the points on the positive slope lines of the instability graph corresponding to W,-1 is related to the delay time T of the feedback channel and the state parameter W. Setting $\alpha=0$ and solving for equations (9) and (10), we obtain the graph of the boundary of the instability domain as shown in Figure Three. Within the domain to the lower left of the solid line, the

value of α is always less than zero. This is the stability domain. At any point to the upper right of the solid line, the eigenvalues contain at least one eigenvalue where α is greater than zero, this is the instability domain. The dotted line in Figure Three denotes the range of values for W. We can see that the graph of the boundary of the instability domain of the Bragg Acousto-optic bistability system differs quite greatly from graph of the boundary of the instability domain of electro-optic bistability systems[6].

Fig 3. The Boundary of the Instability Domain.

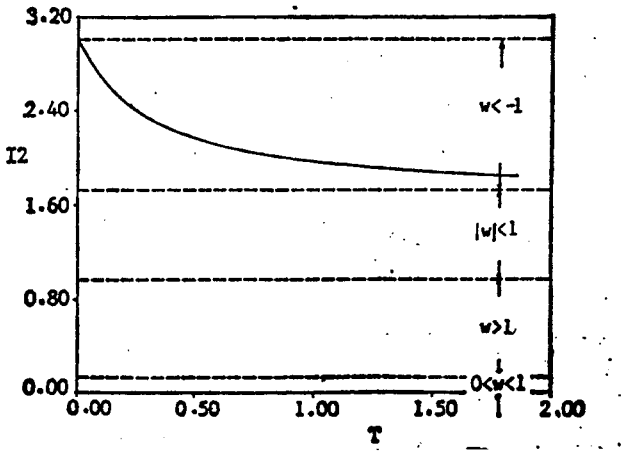

The parameters are K=0, $\theta=0.4V_{\pi}$. Solid curve is boundary of the instability domain. Dashed line shows region of parameter value W.

IV: MODULATION EFFECT

In the system in Figure One, if the intensity of the input light is modulated to a simple harmonic of a certain frequency, then on the basis of the above analysis, we discover that certain extremely interesting modulation effects occur in this system.

1. THE MODULATION EFFECT WITHIN THE STABILITY DOMAIN

In the domain where W<-1 and α<0, that is within the stability domain of the system, when the simple harmonic modulation is performed on the input light intensity corresponding to certain

points on the bistability graph, then

$$I_1(t) = I_0 + A\cos(\omega_0 t), \tag{12}$$

Equation (5) becomes

$$dV(t)/dt + V(t) = g(t), \tag{13}$$

$$g(t) = [I_0 + A\cos(\omega_0(t-T)]K\sin^2[V(t-T)+\theta]. \tag{14}$$

When modulation amplitude A is very small, it can be demonstrated that

$$V(t) \approx V_0 + B\cos(\omega_0 t + \varphi), \tag{15}$$

here, $V_0 = I_0 K \sin^2[V_0+\theta]$, B, and φ are the factors of the modulation frequency ω_0, the modulation amplitude A and other parameters. We can see from this that within the stability domain of this system, when the input light is modulated by a simple harmonic at ω_0, the output is also oscillated at a simple harmonic of ω_0. To study how the simple harmonic output varies with the simple harmonic frequency, we set $\Delta V = V(t)_{max} - V(t)_{max}$ and use a computer to solve for equation (13) and graph Δ against ω_0. By doing this we obtain the four graphs shown in Figure Four of different modulation amplitude A values. Just as predicted, when the modulation frequency and the imaginary part of the linearized eigenvalue (β=6.10) approach each other, there is a peak in output amplitude. This is caused by the modulation signal being a harmonic of one of the eigenvalues of the system. We can also see from the four graphs in Figure four that as modulation amplitude A increases the harmonic peak is lower and shifted to one side. This is obviously the result of the nonlinear response of the system gradually intensifying as the modulation amplitude increases.

Fig 4. Funcion of Amplitude of Output Intensity vs. Modulation Fequency of Iput Itensity in Stable Region, when Input Intensity Is Modulated.

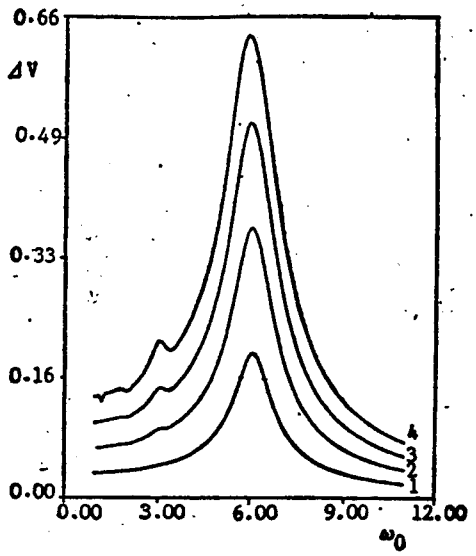

Parameters are K=0.8, $\theta=0.04\pi$, $I_2=2.3$, T=0.27. The imaginary part of the linearized eigenvalue is ß=6.10. Curves 1, 2, ,3, and 4 correspond to A=0.3, 0.6, 0.9 and 1.2.

2. MODULATION EFFECTS IN THE NON-STABLE DOMAIN

In the domain of W<-1 and $\alpha>0$, which is the non-stable domain of the system, when the input light intensity corresponding to a certain point on the bistability graph undergoes simple harmonic modulation in the form of equation (12), the solution to equation (5) may be written as

$$V(t)=V(t=0)e^{-t}+\int_0^t dt' e^{-t(-t')}g(t'), \quad (16)$$

In this equation, the specific form of g(t') is provided by equation (14). Obviously, in this domain the response of the system to the modulation signal will be more complex than the response in the stability domain. Fixing K,θ,A,T,and I_2 and using a solution to compute equation (16), we obtain the values of V(t) for times t. Then using a computer for rapid Fourier transformation, we obtain the fundamental frequency of output oscillation. Then drawing a graph of the fundamental output frequency as a factor of ω_o we obtain Figure Five. We can see from

Figure Five and its corresponding data that on the solid line AB the system output oscillation frequency ω is equal to the input modulation frequency, and system eigenvalue of the fundamental frequency of the output oscillation of $\omega(A=0)=3.12$ falls within this range. This indicates that there are frequency locking phenomena existing near the eigenvalue of the fundamental frequency, and the output light non-linear oscillation is tightly locked in on the input modulation frequency. In Figure Five, the lines CD, EF, GH, IJ, and KL are all frequency lock regions.

Fig. 5. The Function of the Fudamental Frequency of the Output Intensity ω vs. the Modulation Frequency of the Input Intensity ω_o in the Unstable Region.

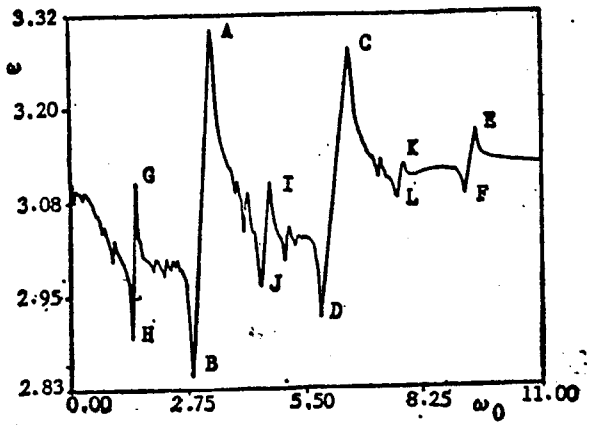

Parameters are K=), $\theta=0.04\pi$, $I_2=2.3$. The eigenvalue of the fundamental frequency of the output intensity is $\omega(A=0)=3.12$, while the imaginary part of the linearized eigenvalue is $\beta=3.36$.

However, within these regions, the input modulation frequencies are 2, 3, 1/2, 3/2, and 5/2 times that of these output oscillation frequencies respectively. Within the non-locked regions in Illustration Five, the relationship between the fundamental output frequency and the input modulation frequency is extremely complex.

The size of the locked regions mentioned above will expand as the modulation frequency A is increased. Figure Six shows the

fundamental frequency locked region AB as modulation amplitude A changes. In this figure, ω_{max} and ω_{min} represent the maximum and minimum frequency respectively of that locked region.

Fig 6. The Function of the Maximum ω_{max} and Minumum ω_{max} of frequency locked region AB in Fig. 5 vs. The Modulation Depth A. $\Delta\omega=\omega_{max}-\omega_{min}$ is frequency locked region AB.

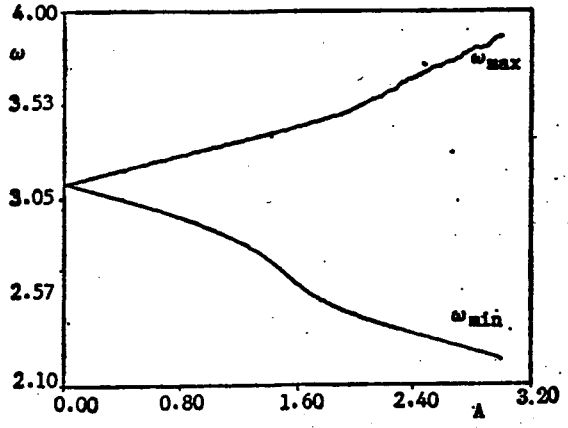

Parameters are K=0.i, θ=o.04π, I_2=2.3, T=0.6, ω(A=0)=3.12, β=3.36.

In frequency locked region AB, fixing the input light modulation frequency ω_o and gradually increasing the modulation amplitude, the system amplitude wave form over time will have sequential multiple cycle, forked circuits, chaotic states, and reverse forked circuits. In order to recognize the forking and chaotic behavior of oscillation wave forms, we conducted Fourier frequency spectrum analysis of each output wave form, the results of which are shown in Figure Seven.

Fig. 7: Function of Fundamental Frequency ω of Output Intensity vs. the Modulation depth A when Modulation Frequency of Input Intensity ω_o is a Constnt in the Frequency in the Locked Region AB of Fig. 5.

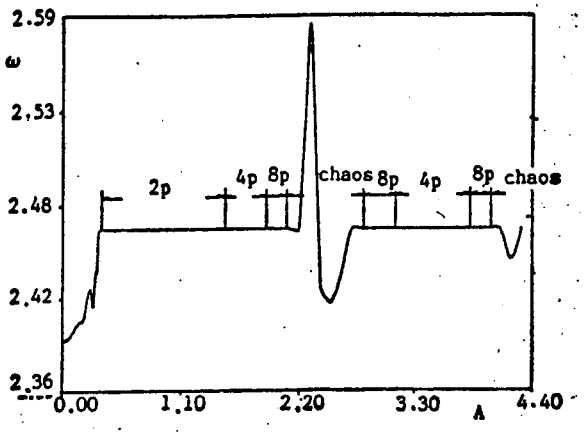

The straight lines running parallel to the abcissa show the frequency lockig phenomenon, where $\omega=\omega_o$, 2p, 4p, and 8p correspond to one, two and three period doubling bifurcations. The parameters are K=0.8, $\theta=04\pi$, $\omega_o=2.46$ $I_2=2.3$, T=0.81, $\omega(A=))=2.39$, ß=2.63.

We can see from this illustration that in order to achieve frequency locking, the modulation amplitude must be exceed a certain minimum threshold. With the exception of the chaotic region, even though threshold exceeding wave form may go through multiple cycle and forking processes, its fundamental frequency of oscillation will always remain locked onto the modulation frequency. This differs from some non-linear systems where the fundamental frequency continues to change in forking processes.

V: CONCLUSIONS

This article analyzes the conditions of bistability of Bragg acousto-optic bistable systems, and, on the basis of its non-linear boundaries, studies the physical responses of such a system to a simple harmonic modulation signal on the input light. It points the eigenvalue harmonic that exists in that system's stable domains and the frequency locking of unstable domains. it also points out

such modulation effects as multiple cycle, forking and chaotic cycles induced by increasing modulation amplitudes. These theoretical results still need to be demonstrated experimentally.

BIBLIOGRAPHY:

1. J. Chrostowski, et al; Opt. Commun., 1982, 41, No.2 (Mar), 71-74.

2. J. Chrostowski et al; Can. J. Phyus, 1983, 61, No.2 (Feb), 188-191.

3. H. Jerominek, et al; Opt. Commun., 1984, 51, No.1 (Aug), 6-10.

4. Dong Xiaoyi, et al; Journal of Optics, 1985, 5, No.12 (Dec), 1074-1081.

5. Li Yonggui, et al; Journal of Physics, 1983, 32 No.3 (Mar), 301-308.

6. J. Y. Gao, et al; Opt. Commun., 1983, 44, No. 3 (Jan), 201-206.